International Journal of Latest Research in Engineering and Technology (IJLRET)
ISSN: 2454-5031
www.ijlret.com || Volume 12 - Issue 06 || June 2026 || PP. 01-10

A Study of a One-Dimensional Fuzzy Fractional Tumor Model using a Modified Analytical Method

Samaresh Kumbhakar[1], Amit Kumar[2*]
[1]*Department of Mathematics, Sidho-Kanho-Birsha University, Purulia, West Bengal, India*
[2]*Department of Mathematics, Balarampur College, Purulia, West Bengal, India*
**Corresponding Author*
amtkr87@gmail.com

Abstract: The mathematical tumor model is an efficient tool for analyzing the tumor growth and propagation. It also helps to plan the treatment in a more accurate way. The net killing rate of tumor cells helps to monitor the growth or decay of the tumor. In this article, two types of one-dimensional time-fractional tumor model is taken based on two types of net killing rate. In addition, fuzzy initial condition is considered. The solution is obtained by the use of an analytical method called the optimal homotopy asymptotic laplace transform method (OHALTM). Numerical experiments are given for both cases to validate the new approach. The small margin of absolute errors shows the accuracy of the solutions. The fractional derivative with fuzzy initial conditions in the tumor model is also discussed.

Keywords: Tumor model, Fractional differential equations, Optimal homotopy asymptotic laplace transform method, Fuzzy initial condition.

1. Introduction

A tumor is a dynamical system in which cancer cells grow and affect other parts of the body. Tumor scan be classified into many types, including brain tumors, bone tumors, lung tumors, pancreatic tumors, and others. It destroys good cells by lowering the level of oxygen and nutrients in the blood.Therefore, understanding tumor dynamics has opened up a huge opportunity for biological, medical researchers, and mathematicians as well. The researchers developed different approaches to discuss tumor growth and treatment outcomes. Among them, mathematical modelling has been shown to be a successful tool to provide an analytical framework of the elements of the immune system involved in cancer treatment. The first mathematical model that studied cancer treatment was developed by Gompertz in 1825. His model includes tumor cell proliferation and death. Later, mathematical models were formulated that describe the interactions of different elements in the tumor microenvironment [1–3]. Within the tumor microenvironment, immune cells, cytokines, chemokines, hormones, and tissue cells are found. Understanding these cell interactions is important for designing better tumor treatment. In addition, real data should be modelled with the highest possible accuracy. From this point of view, fractional differential equations(FDE) areutilize deffectively in a wide range of biological systems [4–6]. FDEs in tumor modelling allow researchers to better realize tumor cell progression and tumor immune cell interactions.Iyoila et al. [7] introduced a time-fractional tumor model based on different types of tumor cell killing rates.

The net killing rate provides information about the growth or decay of the tumor.This could help researchers to achieve a more realistic and holistic description of tumor behavior and choose a particular treatment profile. Anone-dimensional tumor model was introduced by Benzekry et al. [8] to examine cancer cell proliferation using a growth equation with multiple assumptions of constantrate. Moyo et al.[9] investigated a one dimensional tumor model with a variable killing ratio. Aliet al. [10] discussed this tumor model in which the killing ratio varies with the concentration of tumor cells. In our paper, we explored two fractional tumor models based on two types of therapy dependent killing ratio.

$$\frac{\partial^{\upsilon} q(\chi,t)}{\partial t^{\upsilon}} = \frac{\partial^2 q(\chi,t)}{\partial \chi^2} - t^2 q(\chi,t), \tag{1}$$

$$\frac{\partial^{\upsilon} q(\chi,t)}{\partial t^{\upsilon}} = \frac{\partial^2 q(\chi,t)}{\partial \chi^2} - \frac{2}{\chi}\frac{\partial q(\chi,t)}{\partial \chi} - q(\chi,t)^2. \tag{2}$$

Here, $q(\chi,t)$ is the concentration of tumor cells. We use the fractional derivative in the Caputo sense. In Eq.(1), the killing ratio depends only on time and in Eq.(2), the killing ratio varies with the concentration of tumor cells.

Most real life phenomena contain uncertainties and occur across various fields, including medicine, physics, chemistry, engineering, and others. This fuzziness may arise while collecting and measuring data. It

may also arise at the time of formulation of the boundary and initial conditions. As a result, many researchers replaced uncertain crisp quantities with fuzzy quantities that led to fuzzy fractional differential equations [11–13].

In recent years, different homotopy techniques have been widely used in solving linear and non-linear problems. In 1992, Liao [14] proposed the basic ideas of the Homotopy analysis method (HAM) to find analytic solutions to non-linear problems. In 2008, Marinca et al. [15]introduced a new homotopy method called the Optimal homotopy asymptotic method (OHAM) to solve non-linear problems. Later, Azimi et al. [16] applied OHAM to solve strong non-linear differential equations. OHAM reduces the size of the computational domain and is therefore easy to solve. Similarly for HAM, the advantage of OHAM is the integrated convergence criterion. Several articles are present in the existing literature that establish the validity, simplicity, consistency and application of the method in different fields of science [17–19]. In this paper, we extend OHAM to the Optimal homotopy asymptotic laplace transform method (OHALTM) to solve the fuzzy fractional tumor model.

The rest of the paper is constructed as follows: Some definitions related to this work are given in section2. Application of tumor modelling in industrial engineering is discussed in section 3. In section4, the outline of OHALTM is discussed. Some theoretical analysis are done in section 5. Next, the analytical solutions of two types of fuzzy fractional tumor models are obtained in section 6. Graphical representations and numerical discussions are given in section 7 to validate the method. Final remarks are provided in section 8.

2. Mathematical Preliminaries

In this part, we discuss some basic definitions related to fractional derivatives and fuzzy mathematics.

Definition 1: A fuzzy function is defined to be a mapping $\omega : \tau \to E^1, \tau \subseteq E^1$ and ϑ set is: [20]

$$[q(t)]_\vartheta = [\underline{q}(\vartheta,t), \overline{q}(\vartheta,t)], \tag{3}$$

where $t \in \tau$ and $0 \le \vartheta \le 1$. E^1 is the set of all fuzzy numbers.

Definition 2: The well-known Caputo fractional derivative of order υ of the fuzzy function $q(\chi,t)$ can be described as: [21]

$$^cD^{\upsilon}_{\chi_0}\tilde{q}(\chi,t) = [\,^cD^{\upsilon}_{\chi_0}\underline{q}(\chi,t), \,^cD^{\upsilon}_{\chi_0}\overline{q}(\chi,t)], \tag{4}$$

where $^cD^{\upsilon}_{\chi_0}\underline{q}(\chi,t) = \frac{1}{\Gamma(n-\upsilon)}\int_{\chi_0}^{\chi}(\chi-\tau)^{n-\upsilon-1}\underline{q}^{(n)}(\tau)d\tau, n-1 \le \upsilon < n$ and $\frac{d^n}{dt^n}\underline{q}, \upsilon = n, n \in$

and $^cD^{\upsilon}_{\chi_0}\overline{q}(\chi,t) = \frac{1}{\Gamma(n-\upsilon)}\int_{\chi_0}^{\chi}(\chi-\tau)^{n-\upsilon-1}\overline{q}^{(n)}(\tau)d\tau, n-1 \le \upsilon < n$ and $\frac{d^n}{dt^n}\overline{q}, \upsilon = n, n \in$

3. Application in Industrial Engineering

Mathematical tumor models are deeply incorporated with industrial engineering. It works as a bridge between biological tumor dynamics and medical treatment procedures. Analysing the biological constraints, engineers design treatment procedures that maximize patient survival rates as well as minimize overall system costs. Tumor models predict how patients will respond to long-term treatment protocols. Engineers model the balancing between tumor chronological structures and oncology workloads. Industrial engineering also models flexible therapeutic processes by adjusting dosing schedule mathematically to demolish tumor cells while minimizing the long-term harm on the surrounding healthy cells. Industrial engineers use the Gompertz growth or logistic growth tumor models as fundamental constraints in optimal control theory. This helps to secedule the amount of dose and planning of chemotherapy or immunotherapy to minimize tumor volume and minimize the overall toxicity. [22, 23]

Cancer is one of the main causes of death nowadays. Mortality due to cancer can be reduced if tumors are detected earlier so that treatment is started at a less aggressive stage. Also, the refinement in cancer screening, treatment and care is equally important. To enable suitable screening strategies for any cancer type, mathematical models are designed for quantifying the benefits of screening strategies. Tumor treatment immune-therapies require a highly optimized supply chains. Analyzing mathematical tumor models, engineers can predict pharmaceutical demand. This helps the medicine distribution networks to ensure treatments reach patients. Engineers also develop an optimization plan to control appointment queues based on the biological natures of the tumor, substituting traditional chronological sequencing. [24, 25]

4. Optimal Homotopy Asymptotic Laplace Transform Method for fuzzy fractional differential equation

To outline the OHATM process, we take a nonlinear differential equation of the form

$$M(\tilde{q}(\chi,t)) + N(\tilde{q}(\chi,t)) + \tilde{a}(\chi,t) = 0, t \in D^1 \tag{5}$$

with $B\left(\tilde{q}, \frac{\partial \tilde{q}}{\partial \chi}\right) = 0, t \in B^1$ (6)

where $\tilde{a}(\chi,t)$ is an analytic function and D^1 is the domain with boundary B^1.

Taking the Laplace transform on both sides of Eq.(5), we get

$$L\{M(\tilde{q}(\chi,t))\} + L\{N(\tilde{q}(\chi,t))\} + L\{\tilde{a}(\chi,t)\} = 0. \tag{7}$$

Condider a homotopy $\tilde{\sigma} : D^1 \times [0,1] \to$ with

$$\begin{aligned} \mathrm{H}(\tilde{\sigma}(\chi,t,l),l) &= (1-l)[L\{M(\tilde{\sigma}(\chi,t,l))\} + L\{\tilde{a}(\chi,t)\}] \\ &\quad - \mathrm{H}(l)[L\{M(\tilde{\sigma}(\chi,t,l))\} + L\{N(\tilde{\sigma}(\chi,t,l))\} + L\{\tilde{a}(\chi,t)\}] = 0 \end{aligned} \tag{8}$$

where $\mathrm{H}(l)$ is a non-zero auxiliary function associated with the embedding parameter l when $l \neq 0$ and $\mathrm{H}(0) = 0$.

When $l = 0$ then $\tilde{\sigma}(\chi,t,0) = \tilde{q}_0(\chi,t)$ and when $l = 1$ then $\tilde{\sigma}(\chi,t,1) = \tilde{q}(\chi,t)$. Thus, the deformation $\tilde{\sigma}(\chi,t,l)$ transforms the initial guess $\tilde{q}_0(\chi,t)$ into the actual solution $\tilde{q}(\chi,t)$ as l progresses from 0 to 1.

Here we can obtain $\tilde{q}_0(\chi,t)$ by placing $\tilde{q} = 0$ in *Eq.(8)* and *Eq.(6).*

$$L\{M(\tilde{\sigma}(\chi,t,l))\} + L\{\tilde{a}(\chi,t)\} = 0,\ B\left(\tilde{q}_0, \frac{\partial \tilde{q}_0}{\partial \chi}\right) = 0. \tag{9}$$

The auxiliary function $\mathrm{H}(l)$ is assumed to be a polynomial function of the embedding parameter l.

$$\mathrm{H}(l) = m_1 l + m_2 l^2 + m_3 l^3 + \cdots, \tag{10}$$

where $m_1, m_2, m_3, \ldots$ are constants. The approximate solution $\tilde{\sigma}(\chi,t,m_1,m_2,m_3,\ldots)$ can beexpressed in a series about l as

$$L\{\tilde{\sigma}(\chi,t,m_1,m_2,m_3,\ldots)\} = L\{\tilde{q}_0(\chi,t)\} + L\left\{\sum_{i=1}^{\infty} \tilde{q}_i(\chi,t,m_1,m_2,m_3,\ldots) l^i\right\} \tag{11}$$

Now we substitute Eq.(11) in Eq.(8) and equate the coefficients of powers of l. Then we have

$$L\{M(\tilde{q}_1(\chi,t))\} + L\{\tilde{a}(\chi,t)\} = m_1 L\{N_0(\tilde{q}_0(\chi,t))\}, \tag{12}$$

$$B\left(\tilde{q}_1, \frac{\partial \tilde{q}_1}{\partial \chi}\right) = 0, \tag{13}$$

$$\begin{aligned} L\{M(\tilde{q}_2(\chi,t))\} - L\{M(\tilde{q}_1(\chi,t))\} &= m_2 L\{N_0(\tilde{q}_0(\chi,t))\} \\ &\quad + m_1[L\{M(\tilde{q}_1(\chi,t))\} + L\{N_1(\tilde{q}_0(\chi,t),\tilde{q}_1(\chi,t))\}], \end{aligned} \tag{14}$$

$$B\left(\tilde{q}_2, \frac{\partial \tilde{q}_2}{\partial \chi}\right) = 0, \tag{15}$$

which implies

$$\begin{aligned} L\{M(\tilde{q}_j(\chi,t))\} &= L\{M(\tilde{q}_{j-1}(\chi,t))\} + m_j L\{N_0(\tilde{q}_0(\chi,t))\} \\ &\quad + \sum_{i=1}^{j-1} m_i[L\{M(\tilde{q}_{j-1}(\chi,t))\} + L\{N_{j-1}(\tilde{q}_0(\chi,t),\ldots,\tilde{q}_j(\chi,t))\}], \end{aligned} \tag{16}$$

where $N_j(\tilde{q}_0(\chi,t),\ldots,\tilde{q}_j(\chi,t))$ is the coefficient of l^j in $N(\tilde{\sigma}(\chi,t,l))$.

Also,

$$L\{N(\tilde{\sigma}(\chi,t,m_1,m_2,m_3,\ldots))\} = L\{N_0(\tilde{q}_0(\chi,t))\} + L\left\{\sum_{i=1}^{\infty} N_j(\tilde{q}_o,\tilde{q}_1,\ldots,\tilde{q}_j) l^i\right\}. \tag{17}$$

By taking the inverse Laplace transform, we can express the approximate solution of Eq.(5) in the form

$$\tilde{q}(\chi,t,m_1,m_2,m_3,...)=\tilde{q}_0(\chi,t)+\sum_{j=1}^{n-1}\tilde{q}_j(\chi,t,m_1,m_2,m_3,...). \quad (18)$$

Since Eq.(5) is in a fuzzy environment, two solutions: $\underline{q}(\chi,t)$ and $\bar{q}(\chi,t)$ can be obtained.

From Eq.(10) and Eq.(5) we get the residual in the following form

$$R_n(\chi,t,m_1,m_2,m_3,...)=M(\tilde{q}(\chi,t,m_1,m_2,m_3,...))+N(\tilde{q}(\chi,t,m_1,m_2,m_3,...))+\tilde{a}(\chi,t). \quad (19)$$

It can be observed that the constants $m_1,m_2,m_3,...$ determine the n-th approximate solution in Eq.(18). To find these constants, different methods, such as the weighted residual least squaremethod (WRLSM), the Galerkin method exist in the literature.We use WRLSM by constructing a function

$$W(m_1,m_2,...,m_n)=\int_{t_1}^{t_2}\int_{\chi_1}^{\chi_2}R_n^2(\chi,t,m_1,m_2,...,m_n)d\chi dt. \quad (20)$$

The constants $m_1,m_2,m_3,...$ are calculated by solving the set of equations

$$\frac{\partial W}{\partial m_1}=\frac{\partial W}{\partial m_2}=\cdots=\frac{\partial W}{\partial m_n}=0.$$

5. Theoretical Analysis

Theorem1: The series solution $\sum_{j=0}^{n-1}\tilde{q}_j(\chi,t)$ defined in *Eq. (17)* of the Eq. (5) and Eq. (6) converges if $\exists\,\lambda\in(0,1)$ such that $\|\tilde{q}_{j+1}\|\le\lambda\|\tilde{q}_j\|\ \forall j>j_0, j_0\in$.

Proof: Let us construct a sequence $\{Q_n\}_{n=0}^{\infty}$ where

$$\tilde{Q}_0=\tilde{q}_0,$$
$$\tilde{Q}_1=\tilde{q}_0+\tilde{q}_1,$$
$$\tilde{Q}_2=\tilde{q}_0+\tilde{q}_1+\tilde{q}_2,$$
$$\cdots$$
$$\tilde{Q}_n=\tilde{q}_0+\tilde{q}_1+\tilde{q}_2+\cdots+\tilde{q}_n.$$

$$\begin{aligned}\|\tilde{Q}_{n+1}-\tilde{Q}_n\|&=\|\tilde{q}_{n+1}\|\\&\le\lambda\|\tilde{q}_n\|\\&\le\lambda^2\|\tilde{q}_{n-1}\|\\&\cdots\\&\le\lambda^{n-j_0+1}\|\tilde{q}_{j_0}\|\end{aligned}$$

For every $r,s\in$, $r\ge s>j_0$, we have

$$\begin{aligned}\|\tilde{Q}_r-\tilde{Q}_s\|&=\|(\tilde{Q}_r-\tilde{Q}_{r-1})+(\tilde{Q}_{r-1}-\tilde{Q}_{r-2})+\cdots+(\tilde{Q}_{s+1}-\tilde{Q}_s)\|\\&\le\|\tilde{Q}_r-\tilde{Q}_{r-1}\|+\|\tilde{Q}_{r-1}-\tilde{Q}_{r-2}\|+\cdots+\|\tilde{Q}_{s+1}-\tilde{Q}_s\|\\&\quad[By\,the\,triangular\,inequality]\\&\le\lambda^{r-j_0}\|\tilde{q}_0\|+\lambda^{r-j_0-1}\|\tilde{q}_0\|+\cdots+\lambda^{s-j_0+1}\|\tilde{q}_0\|\\&=\left(\frac{1-\lambda^{s-k}}{1-\lambda}\right)\lambda^{r-j_0}\|\tilde{q}_0\|\end{aligned}$$

Since λ lies between 0 and 1, $\|\tilde{Q}_r-\tilde{Q}_s\|\to 0\,as\,r,s\to\infty$.

So, the sequence $\{Q_n\}_{n=0}^{\infty}$ is a Cauchy sequence that implies that the series solution $\sum_{j=0}^{n-1}\tilde{q}_j(\chi,t)$ of Eq. (5) and Eq. (6) converges.

Theorem 2: If $\tilde{q}(\chi,t,m_1,m_2,m_3,...)=\tilde{q}_0(\chi,t)+\sum_{j=1}^{n-1}\tilde{q}_j(\chi,t,m_1,m_2,m_3,...)$ is a finite approximate solution and $\tilde{q}_{exact}(\chi,t)$ is the exact solution of Eq. (5) satisfying $\|\tilde{q}_{j+1}\|\le\lambda\|\tilde{q}_j\|\ \forall j>j_0, j_0\in$ where $\lambda\in(0,1)$, then the maximum value of the absolute error is $\left\|\tilde{q}_{exact}(\chi,t)-\sum_{j=0}^{n-1}\tilde{q}_j(\chi,t,m_1,m_2,m_3,...)\right\|\le\frac{\lambda^n}{1-\lambda}\|\tilde{q}_0(\chi,t)\|$.

Suppose that the series $\sum_{j=0}^{n-1}\tilde{q}_j(\chi,t,m_1,m_2,m_3,...)$ is a finite approximate series solution of Eq. (5).

Now,

$$\left\|\tilde{q}_{exact}(\chi,t)-\sum_{j=0}^{n-1}\tilde{q}_j(\chi,t,m_1,m_2,m_3,...)\right\|=\left\|\sum_{j=n}^{\infty}\tilde{q}_j(\chi,t,m_1,m_2,m_3,...)\right\|$$

$$\le\sum_{j=n}^{\infty}\left\|\tilde{q}_j(\chi,t,m_1,m_2,m_3,...)\right\|$$

$$\le\sum_{j=n}^{\infty}\lambda^j\|\tilde{q}_0(\chi,t)\|$$

$$\le\|\tilde{q}_0(\chi,t)\|\lambda^n(1+\lambda+\lambda^2+\cdots)$$

$$\le\frac{\lambda^n}{1-\lambda}\|\tilde{q}_0(\chi,t)\|.$$

Hence, the theorem is proved.

6. Applications and Numerical Experiments

In this part, we have taken two types of fractional FPE with fuzzy initial conditions.

Example 1:

First, we take the one dimensional tumor model of the form [26, 27]

$$\frac{\partial^{\upsilon}q(\chi,t)}{\partial t^{\upsilon}}=\frac{\partial^2\tilde{q}(\chi,t)}{\partial\chi^2}-t^2\tilde{q}(\chi,t), \tag{21}$$

$\chi,t>0, 0<\upsilon\le1$, with initial condition $\tilde{q}(\chi,0)=\tilde{k}(\rho)e^{a\chi}$ [26] where $\tilde{k}(\rho)=(\underline{k}(\rho),\overline{k}(\rho))=(\rho-1,1-\rho)$.

The exact solution of Eq.(21) is given as $\tilde{q}(\chi,t)=\tilde{k}(\rho)\left[e^{a\chi}+\frac{e^{a\chi}a^2t^{\upsilon}}{\Gamma(1+\upsilon)}+\frac{e^{a\chi}a^4t^{2\upsilon}}{\Gamma(1+2\upsilon)}\right]$[26].

The homotopy for OHALTM is taken as

$$\mathrm{H}(\tilde{\sigma}(\chi,t,l),l)=-\mathrm{H}(l)\left[\frac{\partial^2\tilde{q}(\chi,t)}{\partial\chi^2}-t^2\tilde{q}(\chi,t)\right]=0. \tag{22}$$

By applying OHALTM as illustrated in section 4, we get the following:

$$\tilde{q}_1(\chi,t)=\tilde{q}_0(\chi,t)+L^{-1}\left[s^{-\upsilon}L\left\{m_1\left(\frac{\partial^2\tilde{q}_0(\chi,t)}{\partial\chi^2}-t^2\tilde{q}_0(\chi,t)\right)\right\}\right],$$

$$\tilde{q}_2(\chi,t)=\tilde{q}_1(\chi,t)+L^{-1}\left[s^{-\upsilon}L\left\{(m_1+m_1^2+m_2)\left(\frac{\partial^2\tilde{q}_0(\chi,t)}{\partial\chi^2}-t^2\tilde{q}_0(\chi,t)\right)\quad\left(\frac{\partial^2\tilde{q}_1(\chi,t)}{\partial\chi^2}-t^2\tilde{q}_1(\chi,t)\right)\right\}\right],$$

and so on. We calculate the constants $m_1,m_2,m_3,...$ using WRLSM. By putting the values of the constants and the initial conditions, we get the successive iterations as follows.

$$\tilde{q}_1(\chi,t)=\tilde{k}(\rho)e^{a\chi}m_1\left[\frac{a^2t^{\upsilon}}{\Gamma(1+\upsilon)}+\frac{2t^{2+\upsilon}}{\Gamma(3+\upsilon)}\right],$$

$$\tilde{q}_2(\chi,t)=\tilde{k}(\rho)e^{a\chi}[-\frac{a^2t^{\upsilon}m_1}{\Gamma(1+\upsilon)}+\frac{2t^{2+\upsilon}m_1}{\Gamma(3+\upsilon)}-\frac{a^2t^{\upsilon}m_1^2}{\Gamma(1+\upsilon)}+\frac{2t^{2+\upsilon}m_1^2}{\Gamma(3+\upsilon)}+\frac{a^2t^{2\upsilon}m_1^2}{\Gamma(1+2\upsilon)}-\frac{2a^2t^{2+2\upsilon}m_1^2}{\Gamma(3+2\upsilon)}$$
$$-\frac{a^2t^{2+2\upsilon}m_1^2\Gamma(3+\upsilon)}{\Gamma(1+\upsilon)\Gamma(3+2\upsilon)}+\frac{2t^{4+2\upsilon}m_1^2\Gamma(5+\upsilon)}{\Gamma(3+\upsilon)\Gamma(5+2\upsilon)}-\frac{a^2t^{\upsilon}m_2}{\Gamma(1+\upsilon)}+\frac{2t^{2+\upsilon}m_2}{\Gamma(3+\upsilon)}],$$

and so on.

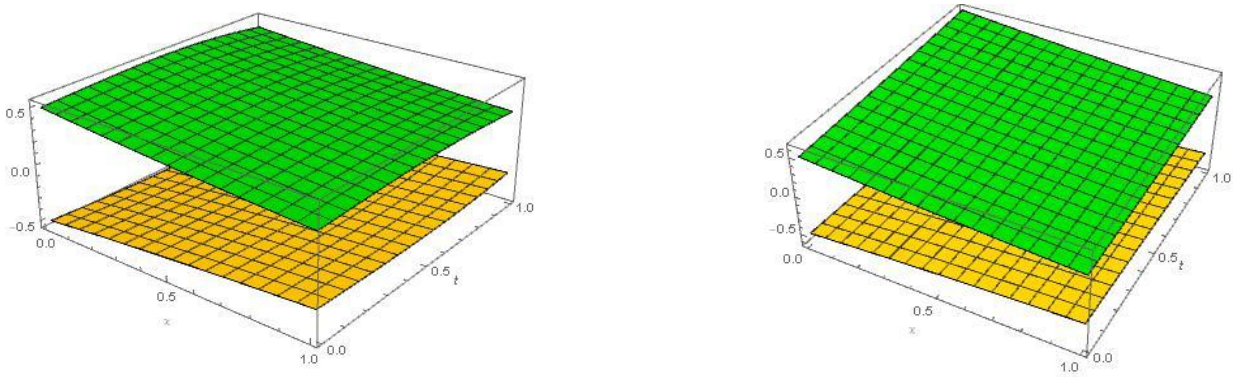

(a) Solutions for $\upsilon=1$ (b) Exact solutions

Fig. 1: Surface plot of the (a) approximate solution and (b) exact solution of Example:1.

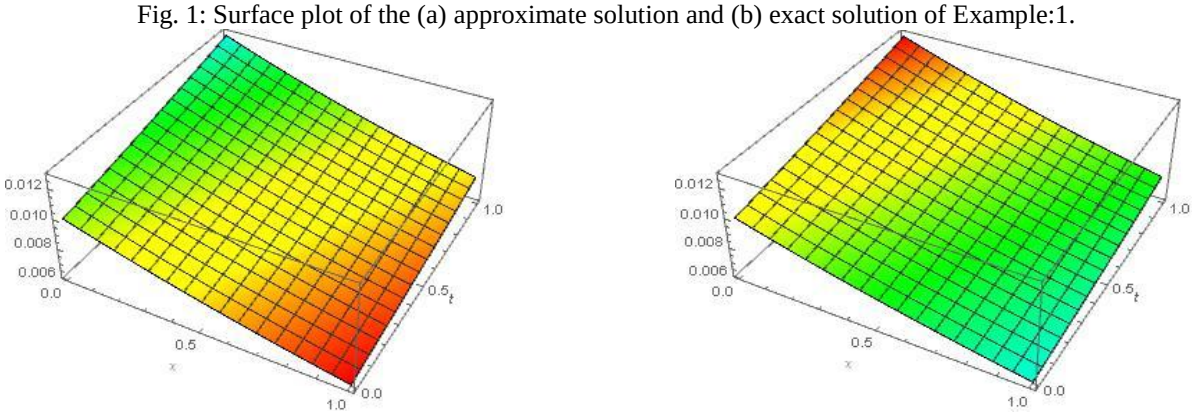

(a) AE in UB solutions (b) AE in LB solutions

Fig. 2: Comparison of the AE in the solutions of Example:1 for (a) UB and (b) LB.

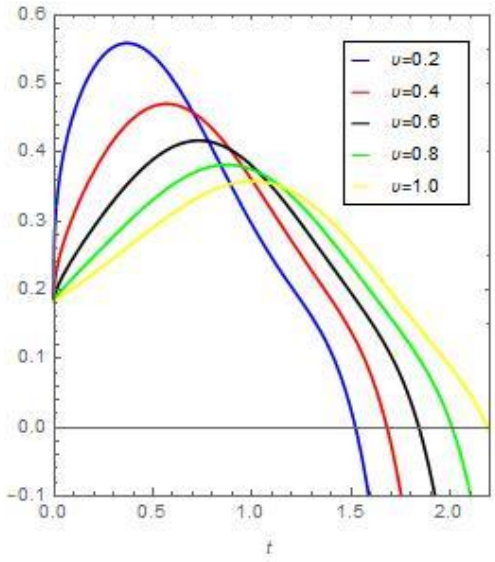

Figure 3: 2D curve of UB solution of Example:1 for different values of **υ**

Example 2:

We take another form of time fractional tumor model as[27]

$$\frac{\partial^{\upsilon}\tilde{q}(\chi,t)}{\partial t^{\upsilon}}=\frac{\partial^{2}\tilde{q}(\chi,t)}{\partial \chi^{2}}-\frac{2}{\chi}\frac{\partial\tilde{q}(\chi,t)}{\partial\chi}-\tilde{q}(\chi,t)^{2}, \tag{23}$$

$\chi,t>0, 0<\upsilon\le 1$ with initial condition $\tilde{q}(\chi,0)=\tilde{k}(\rho)\,\chi^{a}$ [27] where $\tilde{k}(\rho)=(\underline{k}(\rho),\bar{k}(\rho))=(\rho-1,1-\rho)$.

The exact solution of Eq.(23) is given as

$\tilde{q}(\chi,t)=\tilde{k}(\rho)\chi^{-4+a}[-10a^{3}+a^{4}+2\chi^{4+2a}+a^{2}(31-6\chi^{2+a})+6a(-5+2\chi^{2+a})]$ [27].

The homotopy for OHALTM is taken as

$$\mathrm{H}(\tilde{\sigma}(\chi,t,l),l)=-\mathrm{H}(l)\left[\frac{\partial^{2}\tilde{q}(\chi,t)}{\partial\chi^{2}}-\frac{2}{\chi}\frac{\partial\tilde{q}(\chi,t)}{\partial\chi}-\tilde{q}(\chi,t)^{2}\right]=0. \tag{24}$$

By applying OHALTM as illustrated in section 4, we get the following:

$$\tilde{q}_{1}(\chi,t)=\tilde{q}_{0}(\chi,t)+L^{-1}\left[s^{-\upsilon}L\left\{m_{1}\left(\frac{\partial^{2}\tilde{q}_{0}(\chi,t)}{\partial\chi^{2}}-\frac{2}{\chi}\frac{\partial\tilde{q}_{0}(\chi,t)}{\partial\chi}-\tilde{q}_{0}(\chi,t)^{2}\right)\right\}\right],$$

$$\tilde{q}_{2}(\chi,t)=\tilde{q}_{1}(\chi,t)+L^{-1}[s^{-\upsilon}L\{(m_{1}+m_{1}^{2}+m_{2})\left(\frac{\partial^{2}\tilde{q}_{0}(\chi,t)}{\partial\chi^{2}}-\frac{2}{\chi}\frac{\partial\tilde{q}_{0}(\chi,t)}{\partial\chi}-\tilde{q}_{0}(\chi,t)^{2}\right)$$
$$+m_{1}\left(\frac{\partial^{2}\tilde{q}_{1}(\chi,t)}{\partial\chi^{2}}-\frac{2}{\chi}\frac{\partial\tilde{q}_{1}(\chi,t)}{\partial\chi}-\tilde{q}\ (\chi,t)^{2}\right)\}],$$

and so on. We calculate the constants $m_{1},m_{2},m_{3},\ldots$ using WRLSM. By putting the values of the constants and the initial conditions, we get the successive iterations as follows.

$$\tilde{q}_{1}(\chi,t)=\tilde{k}(\rho)\,\chi^{-2+a}m_{1}\left[-\frac{3at^{\upsilon}}{\Gamma(1+\upsilon)}+\frac{a^{2}t^{\upsilon}}{\Gamma(1+\upsilon)}\right]+[\tilde{k}(\rho)]^{2}m_{1}\left[-\frac{t^{\upsilon}\chi^{2a}}{\Gamma(1+\upsilon)}\right],$$

$$\tilde{q}_{2}(\chi,t)=\tilde{k}(\rho)\,\chi^{-2+a}m_{1}\left[\frac{3at^{\upsilon}}{\Gamma(1+\upsilon)}-\frac{a^{2}t^{\upsilon}}{\Gamma(1+\upsilon)}\right]+[\tilde{k}(\rho)]^{2}\chi^{2a}\left[\frac{m_{1}t^{\upsilon}}{\Gamma(1+\upsilon)}+\frac{m_{1}^{2}t^{\upsilon}}{\Gamma(1+\upsilon)}\right]+\tilde{k}(\rho)\,\chi^{-2+a}m_{1}^{2}\left[\frac{at^{\upsilon}}{\Gamma(1+\upsilon)}-\frac{a^{2}t^{\upsilon}}{\Gamma(1+\upsilon)}\right]$$
$$+\tilde{k}(\rho)\,\chi^{-4+a}m_{1}^{2}\left[-\frac{30at^{2\upsilon}}{\Gamma(1+2\upsilon)}+\frac{31a^{2}t^{2\upsilon}}{\Gamma(1+\upsilon)}-\frac{10a^{3}t^{2\upsilon}}{\Gamma(1+2\upsilon)}+\frac{a^{4}t^{2\upsilon}}{\Gamma(1+2\upsilon)}\right]+[\tilde{k}(\rho)]^{2}\chi^{-2+2a}m_{1}^{2}\left[\frac{6at^{2\upsilon}}{\Gamma(1+2\upsilon)}-\frac{4a^{2}t^{2\upsilon}}{\Gamma(1+2\upsilon)}\right]$$
$$+[\tilde{k}(\rho)]^{3}\left[\frac{m_{1}^{3}t^{3\upsilon}\chi^{4a}\Gamma(1+2\upsilon)}{\Gamma(1+\upsilon)^{2}\Gamma(1+3\upsilon)}+\frac{9m_{1}^{2}t^{3\upsilon}\chi^{-4+2a}\Gamma(1+2\upsilon)}{\Gamma(1+\upsilon)^{2}\Gamma(1+3\upsilon)}\right]++[\tilde{k}(\rho)]^{3}\left[\frac{a^{2}m_{1}^{2}t^{3\upsilon}\chi^{-4+2a}\Gamma(1+2\upsilon)}{\Gamma(1+\upsilon)^{2}\Gamma(1+3\upsilon)}\right]$$
$$+\tilde{k}(\rho)\,\chi^{-2+a}m_{2}\left[\frac{3at^{\upsilon}}{\Gamma(1+\upsilon)}\right]+\tilde{k}(\rho)\,\chi^{2a}m_{2}\left[\frac{t^{\upsilon}}{\Gamma(1+\upsilon)}\right]-[\tilde{k}(\rho)]^{2}\chi^{-2+a}m_{2}\left[\frac{a^{2}t^{\upsilon}}{\Gamma(1+\upsilon)}\right],$$

And so on.

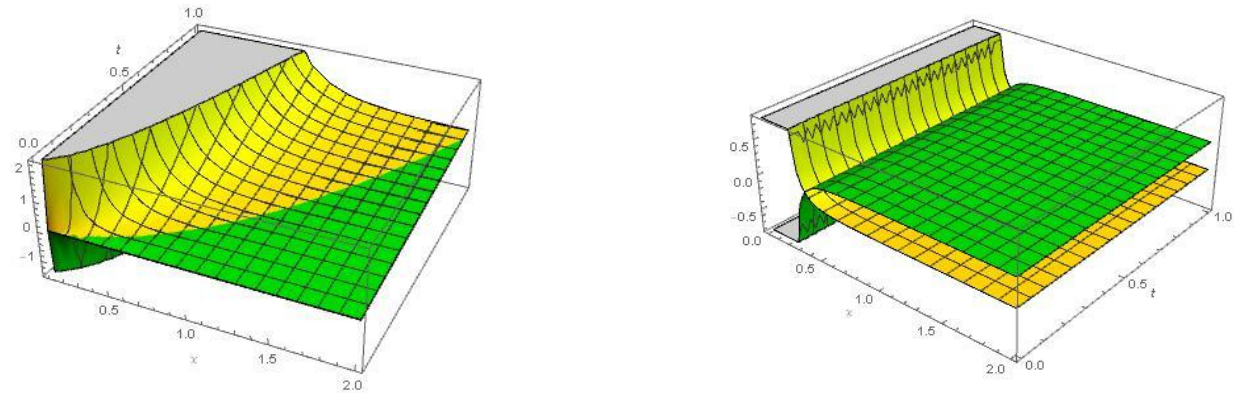

(a) Solutions for $\upsilon=1$ (b) Exact solutions

Fig. 4: Surface plot of the (a) approximate solution and (b) exact solution of Example:2.

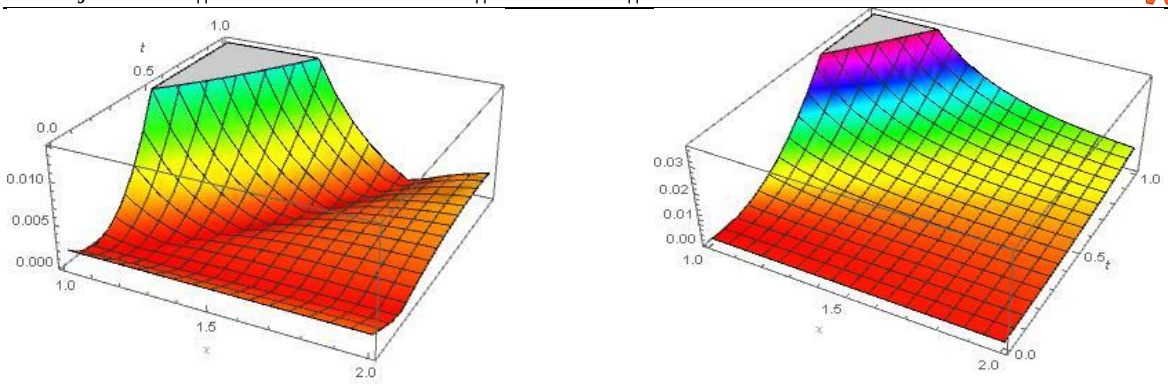

(a) AE in UB solutions (b) AE in LB solutions

Fig. 5: Comparison of the AE in the solutions of Example:2 for (a) UB and (b) LB.

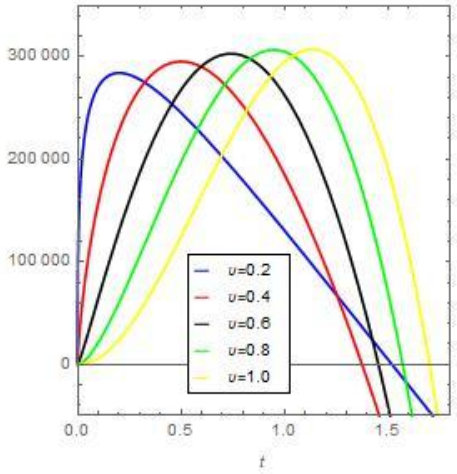

Fig. 6: 2D curve of UB solution of Example:2 for different values of **υ**

7. Numerical Discussions

Fig.1 shows the surface plots of the AS for $\upsilon = 1$ obtained by OHALTM with the exact solutions for example:1. The 3D graphics are drawn at the inflection value $\rho = 0.5$, where the fuzzy LB solution becomes the fuzzy UB solution. The absolute error (AE) $E = |\tilde{q}_{exact}(\chi, t) - \tilde{q}_3(\chi, t)|$ between the exact solution and the third iteration is calculated here. The small margin of the AEs in Fig.2 shows the precision of the solutions. From the 2D curves in Fig.3 we can see that the concentration of cancer cells gradually decreases as time progesses for UB solutions for different values of υ when the net killing rate is solely dependent on time.

In Fig.4, the surface plots of the AS for $\upsilon = 1$ and the exact solutions of example:2 are shown. The 3D graphics exhibit that the solution by the aforesaid method is well-suited to the exact solution.The absolute error curves for the upper and the lower-bound solutions are given in Fig.5. From the 2Dcurves in Fig.6, we can see that when the net killing rate exhibits dependence on the tumor cell concentration,the concentration of cancer cells decreases over time for UB solution for different values of υ.

8. Conclusion

In this article, two types of one-dimensional time-fractional tumor models are analyzed. In the first type, the net killing rate is solely dependent on time, and in the second type, the net killing rate shows dependence on the concentration of tumor cells. Fuzziness in the initial conditions is included. The optimal homotopy asymptotic laplace transform method is used to find analytical solutions of the fuzzy fractional tumor models. Numerical experiments are given for both cases to validate the new approach. The impact of the time-fractional derivative and fuzzy initial conditions on tumor cell concentration is being investigated. Finally, we say that this research is of considerable importance,since this method can be applied to obtain analytic solutions of different tumor models as well as different fuzzy fractional differential equations.

Acknowledgments

The authors are very grateful to the referees for their valuable commentsthat helps us to improve the paper.

Authors Contributaion
Samaresh Kumbhakar: Conceptualization, methodology and software,
Amit Kumar: Visualization, editing.

Funding
This research did not received a grant from any funding agency.

Data Availability
All data supporting the reported findings in this research article are provided in the manuscript.

Conflicts of Interest
The authors declare that they have no conflict of interest.

References
[1] Eftimie, R., Bramson, J.l., & Earn, D.J.D. (2011) Interactions Between the Immune System and Cancer: A Brief Review of Non-spatial Mathematical Models. *Bull Math Biol*, 73: 2–32. DOI: 10.1007/s11538-010-9526-3
[2] Louzoun, Y., Xue, C., Lesinski,G.B., & Friedman, A. (2014) A mathematical model for pancreatic cancer growth and treatments. *Journal of Theoretical Biology*, 351, 74–82. http://dx.doi.org/10.1016/j.jtbi.2014.02.028
[3] Khajanchi, S., & Banerjee, S. (2019) A Strategy of Optimal Efficacy of T11 Target Structure in the Treatment of Brain Tumor.*Journal of Biological Systems*, 27(2) 1–31. DOI:10.1142/S0218339019500104
[4] Kumar, S., Shaw, P. K., Abdel-Aty, A., & Mahmoud, E.E. (2020) A numerical study on fractional differential equation with population growth model. *Numer Methods Partial Differential Eq.*, 1–22. DOI:10.1002/num.22684.
[5] Khan, M. A., & Atangana, A. (2020) Modeling the dynamics of novel coronavirus (2019-nCov) with fractional derivative. *Alexandria Engineering Journal*, 59(4), 2379-2389. https://doi.org/10.1016/j.aej.2020.02.033
[6] Kumar, S., Chauhan, R. P., Abdel-Aty, A., & Abdelwahab, S. F. (2022) A study on fractional tumour–immune-vitamins model for intervention of vitamins. *Results in Physics*, 33, 104963. https://doi.org/10.1016/j.rinp.2021.104963
[7] Iyiola, O.S., & Zaman, F.D. (2014) A fractional diffusion equation model for cancer tumor. *AIP Adv.*, 4, 107121. https://doi.org/10.1063/1.4898331
[8] Benzekry, S., Lamont, C., Beheshti, A., Tracz, A., Ebos, J.M., Hlatky, L., & Hahnfeldt, H. (2014) Classical mathematical models for description and prediction of experimental tumor growth. *PLoS Comput. Biol.*, 10, e1003800. https://doi.org/10.1371/journal.pcbi.1003800
[9] Moyo, S., & Leach, P.G.L. (2004) Symmetry methods applied to a mathematical model of a tumour of the brain. *Proc. Inst. Math. NAS of Ukraine*, 50, 204–210.
[10] Ali, S. M., Bokhari, A. H., Yousuf, M., & Zaman, F. D. (2014) A spherically symmetric model for the tumor growth. *J. Appl. Math.*, 726837. DOI:10.1155/2014/726837
[11] Maitama, S., & Zhao, W. (2021) Homotopy analysis Shehu transform method for solvingfuzzy differential equations of fractional and integer order derivatives.*Computational and Applied Mathematics*, 40:86. https://doi.org/10.1007/s40314-021-01476-9
[12] Almutairi, M., Zureigat, H., Ismail, A. I., & Jameel, A. F. (2021) Fuzzy Numerical Solution via Finite Difference Scheme of Wave Equation in Double Parametrical Fuzzy Number Form. *Mathematics*, 9, 667. https://doi.org/10.3390/math9060667
[13] Verma, V. S., Singh, A., Rana, V., Kaushik, H., & Akgul, A. (2025) Compartmental model analysis for disease dynamics of tuberculosis in fuzzy environment.*Modeling Earth Systems and Environment*, 11:382. https://doi.org/10.1007/s40808-025-02552-3
[14] Liao, S. (1992) The proposed homotopy analysis technique for the solution of nonlinear problems. *PhD thesis, Shanghai Jiao Tong University*.
[15] Marinca, V., Herisanu, N., & Nemes, I. (2008) Optimal homotopy asymptotic method with application to thin flim flow. *Cent. Eur. J. Phys.*, 6(3), 648-653. DOI:10.2478/s11534-008-0061-x.

[16] Azimi, M., Mozaffari, A., & Ommi, F. (2014) Application of galerkin optimal homotopy asymptotic method to shock wave equation.*Journal of Advanced Physics*, 3(1), 35–38. DOI:10.1166/jap.2014.1092.

[17] Mabood, F., Khan, W.A., & Ismail, A.I.M. (2013) Optimal Homotopy Asymptotic Method for Flowand Heat Transfer of a Viscoelastic Fluid in an Axisymmetric Channel with a Porous Wall. *PLOS ONE*, 8(12), e83581.

[18] Gupta, A.K., & Ray, S.S. (2014) On the Solutions of Fractional Burgers-Fisher and Generalized Fisher's Equations Using Two Reliable Methods. *International Journal of Mathematics and Mathematical Sciences*, 2014, 682910. http://dx.doi.org/10.1155/2014/682910

[19] Jameel, A.F., Saaban, A., Altaie, S.A., Anakira, N.R., Alomari, A.K., & Ahmad, N. (2018) Solving first order nonlinear fuzzy differential equations using Optimal homotopy asymptotic method. *International journal of pure and applied Mathematics*, 118(1), 49-64. DOI:10.12732/ijpam.v118i1.5

[20] Sabr, H.A, Abood, B.N., & Suhhiem, M.H. (2021) Fuzzy Homotopy Analysis Method For Solving Fuzzy Riccati Differential Equation. *Journal of Physics: Conference Series 1963*, 012057. doi:10.1088/1742-6596/1963/1/012057

[21] Haq, E. U., Hassan, Q. M. U., Ahmad, J., & Ehsan, K. (2022) Fuzzy solution of system of fuzzy fractional problems using a reliable method. *Alexandria Engineering Journal*, 61, 3051–3058. https://doi.org/10.1016/j.aej.2021.08.034

[22] Yabroff, K. R., Gansler, T., Wender, R. C., Cullen, K. J., & Brawley, O. W. (2019) Minimizing the Burden of Cancer in the United States: Goals for a High-Performing Health Care System. *CA CANCER J CLIN*, 69, 166–183. doi: 10.3322/caac.21556

[23] Magni, P., Simeoni, M., Poggesi, I., Rocchetti, M., & Nicolao, G.D. (2006) A mathematical model to study the effects of drugs administration on tumor growth dynamics. *Mathematical Biosciences*,200(2), Issue 2, 127-151. https://doi.org/10.1016/j.mbs.2005.12.028

[24] Dean, J., Goldberg, E., & Michor, F.() Designing optimal allocations for cancer screening using queuing network models**.** *PLOS Computational Biology*, https://doi.org/10.1371/journal.pcbi.1010179

[25] Safdar, K.A., Emrouznejad, A., & Dey, P.K. (2020) An optimized queue management system to improve patient flow in the absence of appointment system. *International Journal of Health Care Quality Assurance***,** 33(7), 477-494**.** DOI 10.1108/IJHCQA-03-2020-0052

[26] Zureigat, H., Al-Smadi, M., Al-Khateeb, A., Al-Omari, A., & Alhazmi, S. (2023) Numerical Solution for Fuzzy Time- Fractional Cancer Tumor Model with a Time-Dependent Net Killing Rate of Cancer Cells.*Int. J. Environ. Res. Public Health*, 20, 3766. https://doi.org/10.3390/ijerph20043766

[27] Korpinar, Z., Inc, M.,Hıncal, E., & Baleanu, D. (2020) Residual power series algorithm for fractional cancer tumor models.*Alexandria Engineering Journal*, 59, 1405–1412